An Assessment System for Post-Stroke Manual Dexterity Using Principal Component Analysis and Logistic Regression

Bor-Shing Lin, *Member, IEEE*, I-Jung Lee, Pei-Chi Hsiao, and Yi-Ting Hwang

***Abstract*— Hand function assessment is crucial for patients with stroke, who must perform regular repetitive tasks during rehabilitation. However, the conventional evaluation method is subjective and not uniform among physicians. A novel method is proposed in this paper to analyze raw data from a data glove equipped with 16 six-axis inertial measurement units. The proposed method can provide accurate assistance to physicians and objectively assess patients' hand function. Three tasks (the thumb task, the grip task, and the card-turning task) were conducted to evaluate participants' hand function. Representative parameters of hand function in each task and overall evaluation were extracted through principal component analysis and used to develop logistic regression models. The results revealed that all three tasks can be used to perfectly predict healthy subjects and subjects with stroke, with the thumb task exhibiting the highest predictive accuracy for the severity of hand dysfunction. Overall, the proposed method can serve as an efficient method for physicians to assess the hand function of patients with stroke.**

***Index Terms*— Data glove, hand function evaluation, logistic regression, principal component analysis, stroke.**

I. Introduction

STROKE is the primary cause of hand function impairment. From 2003 to 2013, approximately 795 000 people experienced strokes (for the first time or recurrent strokes) [1].

Manuscript received March 15, 2019; revised May 14, 2019; accepted July 9, 2019. Date of publication July 15, 2019; date of current version August 7, 2019. This work was supported in part by the Ministry of Science and Technology in Taiwan, under Grant MOST 107-2221-E-305-014 and Grant MOST 108-2314-B-305-001, in part by the Faculty Group Research Funding Sponsorship by National Taipei University, under Grant 2018-NTPU-ORDA-04 and Grant 2019-NTPU-ORDA-03. *(Corresponding author: Bor-Shing Lin.)*

B.-S. Lin is with the Department of Computer Science and Information Engineering, National Taipei University, New Taipei 23741, Taiwan (e-mail: bslin@mail.ntpu.edu.tw).

I.-J. Lee is with the Department of Computer Science and Information Engineering, National Taipei University, New Taipei 23741, Taiwan, and also with the College of Electrical Engineering and Computer Science, National Taipei University, New Taipei 23741, Taiwan (e-mail: akino_sumiko@hotmail.com).

P.-C. Hsiao is with the Department of Physical Medicine and Rehabilitation, Chi-Mei Medical Center, Tainan 71004, Taiwan (e-mail: peichi1227@gmail.com).

Y.-T. Hwang is with the Department of Statistics, National Taipei University, New Taipei 23741, Taiwan (e-mail: hwangyt@gm.ntpu.edu.tw).

Digital Object Identifier 10.1109/TNSRE.2019.2928719

Patients with stroke and hand function impairment require regular rehabilitation to recover. Meanwhile, physicians regularly observe the hand function of such patients to assess their hand function ability and modify recovery plans based on patients' hand function ability.

A physician uses conventional functional scales to assess the quality of a patient's movement when the patient performs repetitive movement tasks. Brunnstrom stages (BSs), which use six levels to represent the condition of a patient's hand function, are one of the most common clinical methods for assessing the severity of hand impairment [2]. Although conventional scales are widely used, they are subjective and are not uniform among physicians. The ceiling effect can occur as a result of limited scales, which can affect a physician's diagnosis. Thus, measurement errors can occur when a patient's condition is between two BSs. Therefore, an objective and accurate quantitative assessment method is required to overcome the limitations of conventional scales.

Many quantitative assessment methods involving the use of customized tools for the upper limbs and hands of patients with stroke have been proposed. In 2014, Lee *et al.* proposed a smartphone-centric system to measure the range of motion and evaluate the joint condition of patients with stroke [3]. In 2016, Venkataraman *et al.* proposed a camera-based system to extract crucial features from the motion data of patients with stroke and predict movement quality scores [4]. These studies have provided quantitative methods to accurately evaluate the range of motion and quality of movement; however, these methods are suitable only for wide-joint measurement, which means they are unsuitable for finger-joint assessment.

Several studies have used various tools to quantify finger movement quality. Most of these studies have focused on finger movement quality for Parkinson's disease [5]–[8], and they have quantified finger condition by extracting related features when patients with Parkinson's disease perform finger tapping or other evaluation tasks. These studies have provided complete and valuable quantification methods to assess patients' finger conditions. However, these methods are only applicable to Parkinson's disease symptoms. Several studies have provided customized tools or methods to quantify finger movement quality. In 2015, Térémetz *et al.* developed a finger force manipulandum to measure the power of the index,

middle, ring, and little fingers [9]. However, measuring only finger power is inadequate for hand function quantification. With advancements in technology, several sensors have been developed and applied in the rehabilitation domain. Data gloves consisting of various types of sensors have been proposed to evaluate the hand function of patients with stroke. In 2014, Kortier *et al.* developed a sensor glove equipped with inertial measurement units (IMUs) to accurately quantify finger-joint condition [10]. In 2016, Zheng *et al.* presented a data glove equipped with bend sensors and force-sensing resistors to measure joint angles and finger pressure [11]. These two studies have demonstrated the reliability of their respective systems; however, they have focused on verifying system reliability but have not provided quantitative methods or revealed specific features of hand function. In 2012, Oess *et al.* proposed a sensor glove that consisted of flex sensors using quantitative methods to assess the hand function of patients with stroke [12]. In 2016, Yu *et al.* proposed a remote quantitative Fugl–Meyer assessment framework for such patients [13]; this framework extracted five types of features from each sensor and predicted Fugl–Meyer scores. These studies proposed novel methods to quantify the hand function of patients with stroke; however, both studies only used finger-joint angles for assessment and did not provide any parameters to represent detailed information regarding the hand function of patients with stroke. In 2017, Lin *et al.* proposed a data glove equipped with six-axis IMU sensors to assess the hand function of patients with stroke. Three parameters—ARS, VMCT, and QM—were extracted, and k-means was applied to classify patients' BSs [14]. Although this system can classify patients' BSs, it uses only a few motion parameters and may ignore crucial information.

This study developed a method to analyze raw data from a data glove equipped with six-axis IMUs and extracted representative parameters of hand dexterity from three self-defined tasks to evaluate the hand function of patients with stroke. Compared with the previous study [14], the new approach has two main advantages. First, in the previous method, three parameters are extracted by observing the characteristics of each task's signal. However, using only three parameters to represent the performance of manual dexterity is insufficient and may lead to information loss. Therefore, a robust approach based on statistical theory was adopted in the present study to extract and select all possible parameters from each task. Second, in the previous approach, only three parameters are proposed to perform clustering. By contrast, in addition to considering all possible parameters, the present study involves more criteria, including the most influential sensor positions and tasks. Thus, physicians can assess each patient's manual dexterity efficiently in future research by adopting the key criteria presented in this paper.

II. Method

A. Participants

In this study, 15 patients with stroke ("SPs" hereafter; nine male patients and six female patients, mean age: 59.3 ± 16.3 years), comprising four SPs in the fourth BS (BS4), ten SPs in the fifth BS (BS5), and one SP in the sixth BS (BS6), and 15 healthy elderly individuals ("HSs" hereafter; five male individuals and ten female individuals, mean age: 62.6 ± 12.6 years) were recruited. The age difference between the SPs and HSs was nonsignificant ($p = 0.3648$). The experiment was conducted at Chi-Mei Hospital, Tainan, Taiwan. This research (involving human subjects) was reviewed and approved by the ethics committee of Chi-Mei Hospital (IRB No. 10102-019), and the human participants provided their informed consent.

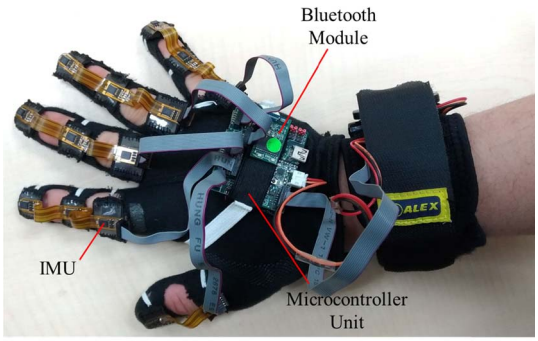

Fig. 1. Photograph of the data glove.

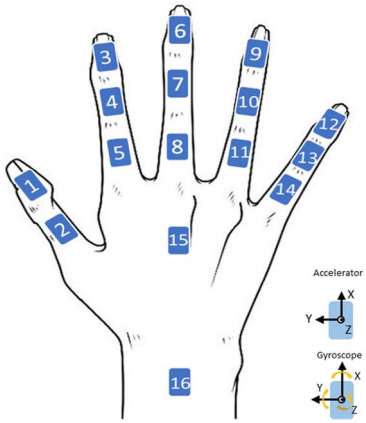

Fig. 2. Positions of the IMU sensors.

B. Data Glove

Participants were asked to wear self-developed data gloves to detect their hands' motion when performing various tasks. Each data glove consisted of 16 IMUs (LSM330DLC, STMicroelectronics, Geneva, Switzerland), and each IMU consisted of a gyroscope and an accelerometer to output three-axis angular velocities and accelerations. A microcontroller unit (MSP430, Texas Instruments Inc., Dallas, TX, USA) was used to collect data from the IMUs and wirelessly transmit the encapsulated packet to a laptop through a Bluetooth interface. Fig. 1 shows a photograph of the data glove, the mechanical design of which was detailed in our previous report [14]. Fig. 2 depicts the positions of the IMU sensors.

C. Experimental Tasks

All participants were asked to perform the following three tasks, namely a thumb task (TT), grip task (GT), and

TABLE I
EXPERIMENTAL PROCESS

Task	Actions	Duration (s)	Cycles
Thumb task (TT)	Press the button Release the button	4 4	10
Grip task (GT)	Grip the tool Release the tool	4 4	10
Card-turning task (CTT)	Turn the card and place it on the table		20

Fig. 3. Cylindrical tool for the TT.

Fig. 4. Tool for the GT.

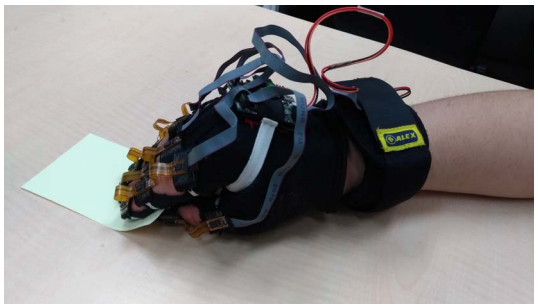

Fig. 5. Card for the CTT.

card-turning task (CTT), which were conducted to evaluate finger and wrist movement quality. Moreover, several scale assessments were conducted by a physician in advance on the SPs to determine their BSs to compare with the evaluation from our proposed system. Table I presents the entire process of the experiments. A detailed description of the experiments is provided in the following section.

D. Clinical Measurements

Physicians graded the hand function of the SPs on the basis of their BSs. One SP was graded as BS6, ten SPs were graded as BS5, and four SPs were graded as BS4. Because SPs with BS6 usually have similar hand function to HSs, the SP with BS6 was categorized as an HS for analysis.

1) TT: The TT was conducted to assess the participants' thumb dexterity. Each participant held a cylinder and repeatedly pushed a button on the cylinder by using their thumb. Fig. 3 displays the cylindrical tool. In the TT, a sound alerted the participant every 4 s to perform the task. One complete motion included pressing and releasing actions. An entire task included ten repetitions of a complete motion and lasted approximately 2 min.

2) GT: The GT was a repetitive finger extension-flexion motion task, which was conducted to evaluate the participants' entire hand dexterity, especially that of the index, middle, ring, little fingers, and wrist. Each participant repetitively performed a grip and release motion by using the tool depicted in Fig. 4. Similar to the procedure in the TT, a sound alerted the participants every 4 s. A complete motion included gripping and releasing; each complete motion was repeated ten times and lasted approximately 2 min, similar to the TT.

3) CTT: The CTT involved repetitive turning of a card to assess the participants' hand mobility and stability. The size of the card used in the task was 7.62×12.70 cm ^{2}, as displayed in Fig. 5. Each participant turned the card 20 times and carefully placed the card to ensure completion of the entire action. The goal of this task was to compare the hand mobility and stability of SPs with those of HSs. The entire motion was repeated 20 times, and the participants were instructed to turn the card as quickly as possible.

E. Data Analysis

In the previous method [14], three parameters, namely ARS, VMCT, and QM, are extracted by observing the characteristics when the SPs and HSs perform the three tasks. However, only the clustering method is used to present the distribution of subjects according to the three parameters. This means that the aforementioned method can only show the clusters using the extracted three features and cannot guarantee the stability and accuracy of assessing the subjects' manual dexterity. Therefore, in the present study, a more robust statistics-based data analysis method was adopted to explore all possible parameters and select the most critical features from the raw data obtained from all IMUs and all tasks. After obtaining all possible significant features, a stable model for manual dexterity assessment could be created using logistic regression (LR).

SAS 9.4 (SAS Institute Inc., Cary, NC, USA) was used to conduct data analysis. Based on the participants' conditions, each participant repeated each task two to five times. Most of the participants repeated the CTT three times. Overall, 111 task recordings were obtained from the HSs and 107 task recordings were obtained from the SPs. In this experiment, 88, 66, and 64 task recordings were obtained from the CTT, GT, and TT, respectively. Data analysis was divided into two parts. The first part classified the HSs and SPs. The data analysis procedure for the first part is presented in Fig. 6. The procedure

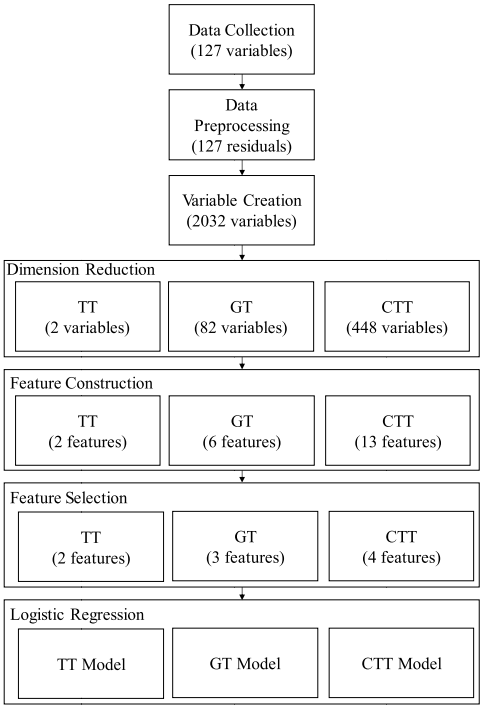

Fig. 6. Data analysis procedure of classifying HSs and SPs.

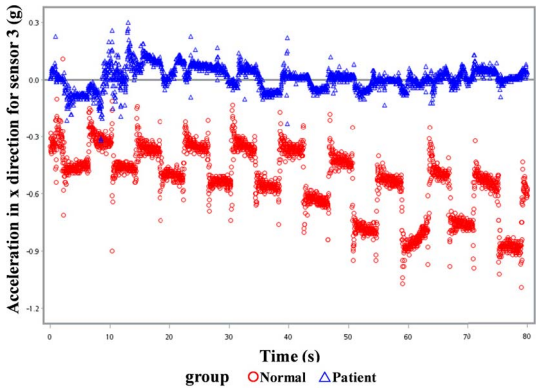

Fig. 7. Acceleration over time in the x-direction for the third IMU sensor during the TT as an example of an upward and downward trend.

included data collection, data preprocessing, variable creation, dimension reduction, feature construction, feature selection, and LR [15].

The second part verified whether the constructed features could be used to classify the severity of the subjects. The Kruskal–Wallis test was used to differentiate severity among features constructed from the feature construction process in the first part.

1) Data Collection: For data collection, 16 IMU sensors were placed on each participant's hand. The acceleration of each sensor was recorded for three directions; thus, 48 acceleration variables were obtained. The change in the total acceleration, which was defined as the square root of the sum of squared acceleration for each direction, was calculated for each sensor, thereby, providing 16 variables. Similarly, for each sensor, the angular velocities were calculated for all three directions. Therefore, 48 angular velocity variables were collected. Every two adjacent sensors incorporated an included angle; thus, the 16 sensors produced a total of 15 angles of finger joints. Overall, 127 variables were collected from each participant.

2) Data Preprocessing and Variable Creation: An upward or downward trend was possible for each variable, as indicated in Fig. 7. A simple linear regression model was used to determine the systematic trend. The estimated intercept and slope were computed for each variable, and the residuals that determined the systematic trend were computed. Four summary statistics, namely the mean, median, standard deviation, and interquartile range for the residuals, were computed for each cycle. Overall, 508 variables were obtained from each participant. Subsequently, the average values (mean and median) of these summary statistics for only the intermediate cycles were computed; the computation yielded 1016 variables. Using these variables calculated from mean and median, the average location and average variation per cycle were obtained. Furthermore, variabilities (standard deviation and interquartile) of the mean and median values of the intermediate cycles were computed; the computation provided 1016 variables. Overall, each task consisted of 2032 variables.

3) Dimension Reduction and Feature Construction: Because each task consisted of 2032 variables, a two-independent-sample t-test was conducted to identify the most crucial variables. A total of 448 and 82 variables of the CTT and GT, respectively, exhibited significant differences in a comparison of the two groups (HSs and SPs). However, for the TT, only two variables that measured the variability of angular velocity in the y-direction from sensor 1 exhibited significant differences in a comparison of the two groups. For the CTT, 57.8% of variables were obtained from angular velocity, 22.3% of variables were obtained from acceleration, 6.9% of variables were obtained from the amount of change of the total acceleration, and 4% of variables were obtained from the joint angles. For the GT, 67.4% of variables were constructed from angular velocity, 18.6% of variables were calculated from acceleration, 7% of variables were obtained from the amount of change of the total acceleration, and 7% of variables were constructed from the joint angles.

Because the variables were highly correlated, principal component analysis (PCA) was employed to construct the features. The number of variables was considerably higher than the number of participants. Before constructing the principal components, a heat map for the correlation of variables, as shown in Fig. 8, was created for identifying the highly correlated variables. Based on the heat map, 13 groups of variables were identified for the CTT, and six groups of variables were identified for the GT. For the CTT, two groups of variables were related to the location and 11 groups of variables were related to the variability of the location. By contrast, for the GT, all six groups of variables were related to the variability.

PCA was then used in each group of variables to construct specific features for the CTT and GT. All extracted components are listed in the appendix. Variables extracted from the CTT were classified into 13 groups. The first group included eight variables, which were obtained from the mean of the

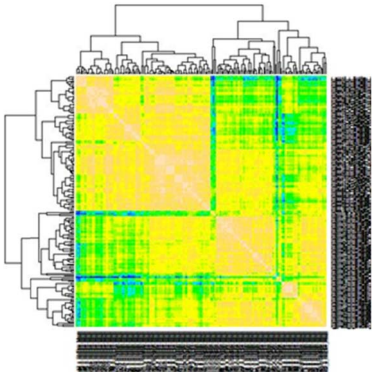

Fig. 8. Heat map based on the correlation of the 530 significant variables in the CTT and GT. 13 groups of variables were identified for the CTT and 6 groups of variables were identified for the GT.

standard deviation per cycle of acceleration in the x-direction of sensors 3, 4, 6, 7, 9, 10, 12, and 13. The component extracted from this group exhibited 98% variance and was named as feature *A*. The second group included 20 variables, which were obtained from the mean of the standard deviation per cycle of acceleration and the amount of change in the total acceleration in the x- and z-directions. In addition to the sensors in feature *A*, the second group included sensors 5 and 11. This group extracted one component, which exhibited 96.7% variance and was named feature *B*. The third group included 12 variables obtained from the mean of the interquartile per cycle of acceleration in the x-direction. The component extracted from this group exhibited 96.8% variance. The component contained all the variables from sensors 3 to 14 and was named feature *C*. The fourth group included 15 variables obtained from the mean of the standard deviation per cycle of acceleration in the y- and z-directions. This component used all the variables from sensors 3 to 14, except sensor 9. This group extracted one component, which exhibited 97.8% variance and was named feature *D*. The fifth group included 27 variables obtained from the mean of the interquartile per cycle of acceleration and the total acceleration in the x-, y-, and z-directions depending on the location of the sensors. This group extracted one component, which exhibited 95.4% variance and was named feature *E*. The sixth group included 42 variables, which were obtained from the mean of the variability per cycle of angular velocity in the x- and z-directions of all sensors except sensors 1 and 16. The component extracted from this group exhibited 93.6% variance and was named feature *F*. The seventh group included 12 variables, which were obtained from the mean of the standard deviation per cycle of angular velocity in the y-direction. The component extracted from this group used the variables obtained from sensors 3 to 14, exhibited 96.4% variance, and was named feature *G*. The eighth group included 23 variables, which were obtained from the variability of the location per cycle of angular velocity in the y-direction. The variables were obtained from sensors 4 to 15. The component extracted from this group exhibited 91.3% variance and was named feature *H*. The ninth group included 20 variables, which were obtained from the variability of the location per cycle of angular velocity in the z-direction. The variables were obtained from sensors 3 to 14. The component extracted from this group exhibited 88.2% variance and was named feature *I*. The tenth group included 18 variables, which were obtained from the variability of the location per cycle of acceleration and the total acceleration in the x-, y-, and z-directions depending upon the location of the sensors. The variables for this component were extracted from sensors 1, 2, 3, 4, 7, 8, 11, 14, and 15. This component exhibited 86.7% variance and was named feature *J*. The eleventh group included 11 variables, which were obtained from the variability of the location per cycle of acceleration in the x-direction. The variables for this component were extracted from sensors 6, 7, 9, 10, and 12. The component extracted from this group exhibited 89.8% variance and was named feature *K*. The twelfth group included 24 variables, which were obtained from the location of the location per cycle of angular velocity in the y-direction. The variables for this component were extracted from sensors 3 to 14. The component extracted from this group exhibited 85.5% variance and was named feature *L*. The final group included four variables obtained from the location of the location per cycle of the angle. The variables for this component were extracted from sensors 8 and 11. The component extracted from this group exhibited 92.9% variance and was named feature *M*.

The variables extracted from the GT were classified into six groups. The first group included ten variables obtained from the mean of the interquartile per cycle of angular velocity in the y-direction. The variables for this component were extracted from sensors 2, 3, 4, 5, 8, and 11 to 15. The component extracted from this group exhibited 96.6% variance and was named feature *N*. The second group included 11 variables, which were obtained from the mean of the interquartile per cycle of angular velocity in the z-direction. The variables for this component were extracted from sensors 3, 4, and 6 to 14. The component extracted from this group exhibited 94.4% variance and was named feature *O*. The third group included 17 variables obtained from the mean of the interquartile per cycle of angular velocity in the x- and z-directions. The variables for this component were extracted from sensors 2, 3, and 6 to 13. The component extracted from this group exhibited 95.2% variance and was named feature *P*. The fourth group included 12 variables, which were obtained from the mean of the standard deviation per cycle of angular velocity in the y-direction. The variables for this component were extracted from sensors 3 to 14. The component extracted from this group exhibited 96.4% variance and was named feature *Q*. The fifth group included 11 variables, which were obtained from the mean of the interquartile per cycle of angular velocity in the y-direction. The variables for this component were extracted from sensors 6 to 15. The component extracted from this sensor exhibited 96.4% variance and was named feature *R*. The final group included 12 variables obtained from the mean of the interquartile per cycle of the angular velocity in the x-direction. The variables for this component were extracted from sensors 5 to 15. The component extracted from this feature exhibited 95.8% variance and was named feature *S*.

4) Feature Selection, LR, and Performance Evaluation: The ability of these constructed features to predict the participants'

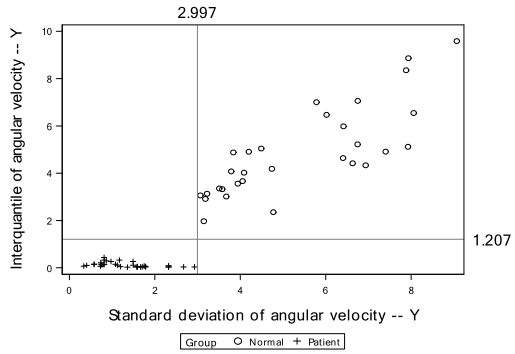

Fig. 9. Scatter plot of standard deviation and interquartile of angular velocity in the y-axis for the TT.

status was assessed using the LR based on data from all three tasks. Backward selection with removal criterion 0.05 was set to select the most influential features. Standardized estimates were used to evaluate the importance of the predictors. The receiving operator characteristic (ROC) curve and the area under the ROC curve (AUC) were computed to evaluate the predictive power of the models. Finally, the Kruskal–Wallis test was employed to investigate the ability of the constructed features in classifying the severity of hand movement dysfunction.

III. Results

A. Classification Between HS and SP

In this experiment, Y denoted the status of the response variable, in which 1 denoted an SP and 0 denoted an HS. In addition, x denoted the vector of the predictor variables in general. The ability to classify the SPs and HSs was evaluated for each task.

1) Results of the TT: Only two variables, standard deviation and interquartile range, that measured the variability of angular velocity in the y-direction from sensor 1 were selected. LR yielded a perfect fit. Fig. 9 presents a scatter plot of variables' standard deviations and interquartile ranges. Based on this scatter plot, the HSs corresponded to high variability, whereas the SPs corresponded to low variability. The scatter plot shows that the threshold between SPs and HSs was 2.997 for standard deviation and 1.207 for interquartile range. This difference clearly distinguishes the two groups.

2) Results of the GT: Six features were identified. LR yielded a perfect fit for P, R, and S. Fig. 10 presents the scatter plots of P, R, and S. Based on the three scatter plots in Fig. 10, SPs have high values of P, R, and S, whereas HSs have small values of P, R, and S.

3) Results of the CTT: Based on the removal criterion 0.05 for the backward selection and using only the recordings from the CTT, features B, C, D, and K were selected from the CTT. LR for this case was calculated according to (1). The selected features for the CTT are listed in Table II.

$$log\left(\frac{P[Y=1|x]}{P[Y=0|x]}\right) = -1.58 - 3.61B + 2.25C + 3.00D - 1.96K. \quad (1)$$

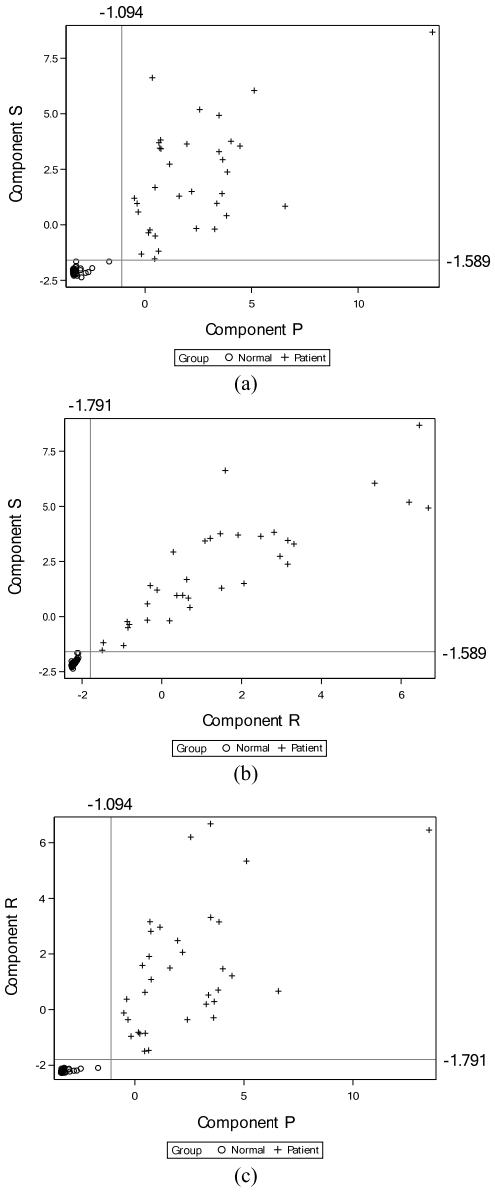

Fig. 10. Scatter plot of features P, R and S for the GT: (a) features P and S, (b) features R and S, and (c) features P and R.

TABLE II
SELECTED FEATURES IN THE CTT MODEL

Feature	Estimate	SE	p	Std Est	c
Intercept	-1.58	0.64	0.014		0.98
B	-3.61	0.94	<.001	-7.76	
C	2.25	0.79	0.004	3.37	
D	3.00	0.78	<.001	5.43	
K	-1.96	0.69	0.005	-2.62	

In the experiment, B and K were negatively associated with the event, whereas C and D were positively associated with the event. B and D were the most influential features. The ROC curve and AUC of the CTT model are presented in Fig. 11, revealing that the predictive power of this model was 0.98.

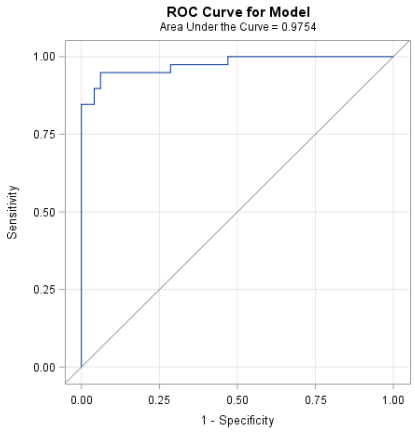

Fig. 11. ROC curve and AUC of the CTT model

B. Classification Based on the Severity of the Subjects

The severity of the disease was measured in terms of BSs. Moreover, SPs were further classified into BS4 and BS5. The variable Z denoted the status of the severity, in which 0 denoted HS, 1 denoted BS5, and 2 denoted BS4. Among 218 recordings, 25 recordings (11.5%) and 75 (34.4%) were collected from BS4 and BS5 participants, respectively. For each task, only nine, eight, and eight recordings were collected from BS4.

The Kruskal–Wallis test was used to compare the three groups. Furthermore, it was used again to compare BS4 and BS5. The results are presented in Table III. These show significant differences in the results of the 13 features extracted from the CTT and 6 features extracted from the GT between the SPs and HSs. Further comparison revealed that the difference in these features between BS4 and BS5 was nonsignificant.

Fig. 12 presents box plots of the selected variables for the three groups while conducting the TT. For the TT, the variable measuring the standard deviation of angular velocity in the y-direction from sensor 1 exhibited considerable differences among the three groups. However, the variable that measured the interquartile range of angular velocity in the y-direction from sensor 1 exhibited a considerable difference between the SPs and HSs but only a small difference between BS4 and BS5.

Table IV compares the previous method [14] with that of the present study. For feature extraction and selection, the previous method mainly obtains features by observing the characteristics of the subjects' movements while they perform the TT, GT, and CTT. However, the proposed method in the present study adopts statistical methods to analyze the raw data and extract all possible features. Next, PCA is adopted to reduce the dimensions of the data set, and the most influential features are selected using backward selection. Therefore, the previous method could not create a stable model for predicting severity, whereas the proposed method can create a stable model with influential features for performing predictions. Regarding the information provided by the two methods, the previous method only provides three features for the overall evaluation, whereas the proposed method provides influential features for each task. Moreover, the most important sensor positions and tasks are provided to enhance the quality and efficiency of future manual dexterity assessment. Therefore, more comprehensive information can be obtained by adopting the proposed method than by adopting the previous method.

IV. Discussion

In this study, three tasks were conducted to evaluate the participants' hand function. PCA was conducted to create specific features for the GT and CTT. The performance and most influential predictor of each task are presented in Figs. 9, 10, and 11 as well as Table II to differentiate between the HSs and SPs. Fig. 9 shows that the standard deviation and interquartile range of angular velocity in the y-axis from sensor 1 were the most influential predictors in the TT. This result indicated that a subject was an SP if the two predictors were low. Moreover, the results indicated that the position of sensor 1 was important for the TT. This is primarily because the two predictors represent the mobility of a subject's thumb, and HSs have higher mobility in their thumbs than that of SPs. Fig. 10 shows that the features P, R, and S were the most important predictors for the GT. Furthermore, this result implied that a participant was an SP if the values of P, R, and S were high. The features P, R, and S were mainly composed of the interquartile range of acceleration in the z-axis and the interquartile range of angular velocity in the x- and y-axis after normalization. Low values of the three features indicated highly stable hand function. HSs demonstrated high stability when the GT was performed and tended to be in a similar range of values because of the normalization; however, SPs exhibited low stability when the GT was performed and were not in a specific range. Table II shows that features B and D were the most influential predictors for the CTT, which implied that a participant was an HS if the value of B was high and that of D was low. Feature B was mainly composed of the average standard deviation of acceleration in the z-axis from the sensors on the index, middle, ring, and little fingers. Feature B represented the hand mobility of the participant when the CTT was performed. Thus, the HSs had higher hand mobility than the SPs did. Feature D mainly consisted of the average standard deviation of acceleration in the y-axis from the whole sensors on the hand except the sensor on the thumb. Moreover, D represented the horizontal tremor of the hand when performing the CTT. This indicates that SPs may have had considerable tremors on their hands when performing the CTT. Overall, the results revealed that the three tasks could accurately differentiate SPs and HSs. Furthermore, classification of SPs and HSs using the TT and GT could attain a predictive power of 1.0, whereas CTT could attain a predictive power of 0.98.

A crucial aspect of the hand function assessment described herein is measuring disease severity. The disease severity calculated from the experiment is presented in Table III. This shows that the three proposed tasks could be used to accurately classify HS, BS4, and BS5; however, for classification of BS4 and BS5, only the standard deviation of angular velocity when conducting the TT could differentiate BS4 and BS5.

TABLE III
SELECTED VARIABLES IN EACH TASK FOR MEASURING DISEASE SEVERITY

Task	Feature	HS Mean	HS STD Error	BS5 Mean	BS5 STD Error	BS4 Mean	BS4 STD Error	p*	p&
TT	QRANGE of angular velocity	4.56	2.19	0.12	0.09	0.19	0.13	<.001	0.082
	STD of angular velocity	5.12	2.04	1.56	0.62	0.62	0.18	<.001	<.001
GT	N	-2.10	0.29	1.51	2.43	1.60	1.13	<.001	0.338
	O	-1.98	0.42	2.11	2.63	2.38	1.46	<.001	0.602
	P	-2.97	0.87	2.21	2.99	3.11	1.61	<.001	0.098
	Q	0.22	0.92	0.81	2.66	1.27	1.74	0.401	0.514
	R	-2.12	0.33	1.53	2.42	1.76	1.56	<.001	0.459
	S	-1.98	0.46	2.13	2.38	2.87	2.54	<.001	0.433
CTT	A	0.71	2.38	-1.93	1.91	-1.99	1.58	<.001	0.869
	B	0.81	3.67	-2.87	3.34	-3.02	2.58	<.001	0.674
	C	0.33	2.94	-1.42	2.11	-1.58	1.49	<.001	0.898
	D	-0.25	3.66	-1.78	2.56	-2.01	1.86	<.001	0.674
	E	-0.42	4.84	-2.02	3.14	-2.08	2.39	<.001	0.869
	F	-0.71	6.17	-2.95	3.93	-1.91	4.63	<.001	0.956
	G	0.18	3.17	-2.55	2.10	-1.96	2.51	<.001	0.956
	H	-0.53	3.07	-2.14	1.37	-1.76	1.89	<.001	0.985
	I	-0.42	3.61	-2.04	1.76	-1.47	2.53	<.001	0.841
	J	-0.53	3.01	-1.55	1.83	-2.08	1.05	0.074	0.756
	K	0.35	2.72	-1.59	1.21	-2.02	0.81	<.001	0.432
	L	-0.53	3.07	-2.14	1.37	-1.76	1.89	<.001	0.985
	M	-0.42	3.61	-2.04	1.76	-1.47	2.53	<.001	0.841

p*means the p value for comparing HS, BS5, and BS4
p& means the p value for comparing BS5 and BS4

p indicates the p value of each feature for comparing HS and SP
c indicates the predictive power of the CTT model

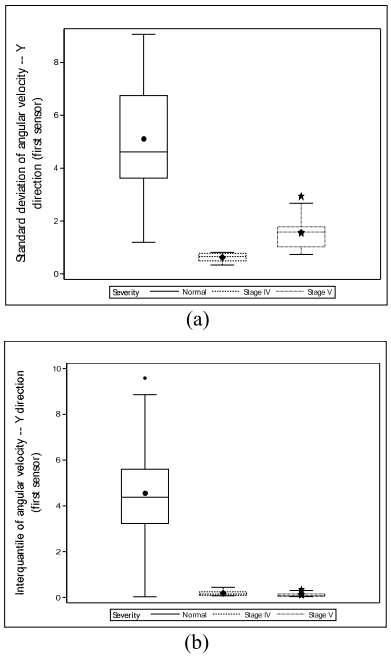

Fig. 12. Box plots of the selected features for the three groups while conducting TT: (a) standard deviation of angular velocity in the y-axis from sensor 1 and (b) interquartile range of the angular velocity in the y-axis from sensor 1.

Box plots presented in Fig. 12 indicate the features from the TT to differentiate HS, BS4, and BS5. The TT was the only task that could accurately differentiate SPs in BS4 and BS5.

TABLE IV
COMPARISON BETWEEN THE PREVIOUS METHOD AND PROPOSED METHOD

	Previous Method	Proposed Method
Feature Extraction and Selection	Observation	Statistical methods and PCA
Stable Model	No	LR
Provide Important Features	3 features	2 features for TT, 6 features for GT, 13 features for CTT
Provide Important Sensor Positions	No	Yes
Provide Important Tasks	No	Yes

However, the TT only provided the features of a thumb. By contrast, the GT and CTT could extract more features of hand function, but the limited samples in BS4 reduced the accuracy of prediction from the GT and CTT when differentiating BS4 and BS5. If the samples of BS4 increased, the performance of the GT and CTT would increase when classifying BS4 and BS5. Therefore, if physicians require additional hand function features, the GT and CTT would be preferable for classifying the severity of hand dysfunction. In the future, the GT and CTT could be used to provide detailed information regarding manual dexterity if more clinical data are collected.

V. Conclusion

In this study, LR was used to analyze raw data from a data glove equipped with six-axis IMUs and to extract the representative hand function parameters. Three tasks—the TT, GT, and CTT—were conducted to evaluate the hand function of patients with stroke. The results revealed that the proposed tasks could be used to accurately differentiate HS and SP. The TT and GT could precisely 100% separate HS and SP, and the CTT reached a predictive power of 0.98. The TT exhibited the most accurate performance in identifying hand dysfunction severity among the participants. Therefore, the TT is the most effective method of differentiating HSs and SPs as well as identifying dysfunction severity.

The lower performance of the GT and CTT in determining dysfunction severity was because of the limited number of BS4 participants. However, the GT and CTT can provide additional manual dexterity information compared with using the TT. Therefore, more participants should be recruited in BS4 in future studies to improve the performance of prediction using the GT and CTT.

References

[1] D. Mozaffarian *et al.*, "Heart disease and stroke statistics-2016 update a report from the American Heart Assoication," *Circulation*, vol. 133, no. 4, pp. e38–e48, Jan. 2016.

[2] K. A. Sawner and J. M. LaVigne, *Brunnstrom's Movement Therapy in Hemiplegia: A Neurophysiological Approach*. Philadelphia, PA, USA: Lippincott, 1992.

[3] W. W. Lee, "A smartphone-centric system for the range of motion assessment in stroke patients," *IEEE J. Biomed. Health Inform.*, vol. 18, no. 6, pp. 1839–1847, Nov. 2014.

[4] V. Venkataraman *et al.*, "Component-level tuning of kinematic features from composite therapist impressions of movement quality," *IEEE J. Biomed. Health Informat.*, vol. 20, no. 1, pp. 143–152, Jan. 2016.

[5] J. Stamatakis, "Finger tapping clinimetric score prediction in Parkinson's disease using low-cost accelerometers," *Comput. Intell. Neurosci.*, vol. 2013, no. 717853, Jan. 2013, Art. no. 1.

[6] H. Dai, H. Lin, and T. C. Lueth, "Quantitative assessment of parkinsonian bradykinesia based on an inertial measurement unit," *Biomed. Eng. Online*, vol. 14, no. 1, Dec. 2015, Art. no. 68.

[7] Y. Sano, "Quantifying Parkinson's disease finger-tapping severity by extracting and synthesizing finger motion properties," *Med. Biol. Eng. Comput.*, vol. 54, no. 6, pp. 953–965, Jun. 2016.

[8] M. Djurić-Jovičić *et al.*, "Finger tapping analysis in patients with Parkinson's disease and atypical parkinsonism," *J. Clin. Neurosci.*, vol. 30, pp. 49–55, Aug. 2016.

[9] H. G. Kortier, V. I. Sluiter, D. Roetenberg, and P. H. Veltink, "Assessment of hand kinematics using inertial and magnetic sensors," *J. Neuroeng. Rehabil.*, vol. 11, no. 1, p. 70, Dec. 2014.

[10] Y. Zheng, Y. Peng, G. Wang, X. Liu, X. Dong, and J. Wang, "Development and evaluation of a sensor glove for hand function assessment and preliminary attempts at assessing hand coordination," *Measurement*, vol. 93, pp. 1–12, Nov. 2016.

[11] M. Térémetz, F. Colle, S. Hamdoun, M. A. Maier, and P. G. Lindberg, "A novel method for the quantification of key components of manual dexterity after stroke," *J. Neuroeng. Rehabil.*, vol. 12, no. 1, Dec. 2015, Art. no. 64.

[12] N. P. Oess, J. Wanek, and A. Curt, "Design and evaluation of a low-cost instrumented glove for hand function assessment," *J. Neuroeng. Rehabil.*, vol. 9, no. 2, pp. 1–11, Jan. 2012.

[13] L. Yu, D. Xiong, L. Guo, and J. Wang, "A remote quantitative Fugl-Meyer assessment framework for stroke patients based on wearable sensor networks," *Comput. Methods Programs Biomed.*, vol. 128, pp. 100–110, May 2016.

[14] B.-S. Lin, P.-C. Hsiao, S.-Y. Yang, C.-S. Su, I-J. Lee, "Data glove system embedded with inertial measurement units for hand function evaluation in stroke patients," *IEEE Trans. Neural Syst. Rehabil. Eng.*, vol. 25, no. 11, pp. 2204–2213, Nov. 2017.

[15] A. Agresti, "Logistic regression," in *Categorical Data Analysis*, 3rd ed. Hoboken, NJ, USA: Wiley, 2012, pp. 163–195.